

## Fluctuation in the Microtubule Sliding Movement Driven by Kinesin in Vitro

Yasuhiro Imafuku,\* Yoko Y. Toyoshima,<sup>†</sup> and Katsuhisa Tawada<sup>§</sup>

<sup>\*</sup>Department of Molecular Biology, Graduate School of Medical Sciences, and <sup>§</sup>Department of Biology, Faculty of Science, Kyushu University, Fukuoka, Fukuoka 812, Japan, and <sup>†</sup>Department of Pure and Applied Sciences, College of Arts and Sciences, University of Tokyo, Komaba, Tokyo 153, Japan

**ABSTRACT** We studied the fluctuation in the translational sliding movement of microtubules driven by kinesin in a motility assay in vitro. By calculating the mean-square displacement deviation from the average as a function of time, we obtained motional diffusion coefficients for microtubules and analyzed the dependence of the coefficients on microtubule length. Our analyses suggest that 1) the motional diffusion coefficient consists of the sum of two terms, one that is proportional to the inverse of the microtubule length (as the longitudinal diffusion coefficient of a filament in Brownian movement is) and another that is independent of the length, and 2) the length-dependent term decreases with increasing kinesin concentration. This latter term almost vanishes within the length range we studied at high kinesin concentrations. From the length-dependence relationship, we evaluated the friction coefficient for sliding microtubules. This value is much larger than the solvent friction and thus consistent with protein friction. The length independence of the motional diffusion coefficient observed at sufficiently high kinesin concentrations indicates the presence of correlation in the sliding movement fluctuation. This places significant constraint on the possible mechanisms of the sliding movement generation by kinesin motors in vitro.

### INTRODUCTION

With a recently developed in vitro motility assay, it has become possible to study the sliding movements of individual cytoskeletal filaments generated by protein motors under well defined conditions (Kron and Spudich, 1986; Harada et al., 1987; Vale and Toyoshima, 1988; Howard et al., 1989). Fluctuations in the sliding movement of individual filaments provide information about the dynamic aspects of the mechanisms responsible for the generation of the movement by protein motors (Svoboda et al., 1994). However, detailed analyses of the fluctuation of the sliding movements under no external load have not hitherto been made.

In this study we examined the fluctuations in the movement of individual microtubules sliding over kinesin in vitro, by calculating the mean-square deviation of the sliding displacement from the average (Qian et al., 1991). The mean-square displacement deviation from the average as a function of time interval yields a diffusion coefficient of a filament, which will herein be referred to as the motional diffusion coefficient. This is a measure of the fluctuation of the movements, analogous to the diffusion coefficient observed for thermally generated or protein motor-mediated Brownian movement (Vale et al., 1989; Berg, 1993). The length dependence of the longitudinal diffusion coefficient of a filamentous particle in Brownian movement provides us with information about the characteristics of the interactions between the fila-

ment and the particles that cause its Brownian movement. The dependence of the motional diffusion coefficient on the filament length will likewise provide us with information about some characteristics of the interaction of the protein motors with a sliding filament.

With these approaches, we found that 1) the motional diffusion coefficient primarily decreased (but did not go down asymptotically to zero) with increasing the microtubule length and 2) the relationship between the motional diffusion coefficient and the microtubule length depended upon the kinesin concentration: the higher the kinesin concentrations, the smaller the dependence of the motional diffusion coefficient on the microtubule length. Finally, the motional diffusion coefficient depended little upon the microtubule length in the range we studied, when the concentration of kinesin was sufficiently high. From the length dependence of the motional diffusion coefficient, we evaluated the friction coefficient and found that it was more than 100 times larger than the solvent friction. This relatively large value is thus consistent with protein friction (Tawada and Sekimoto, 1991b).

The length independence of the motional diffusion coefficient observed at sufficiently high kinesin concentrations contrasts sharply with the inverse proportionality of the length dependence of the diffusion coefficient in Brownian movement. The inverse proportionality of the latter is a direct consequence of the central limit theorem, with the premise that the action of particles causing Brownian movement of a filament is random (i.e., stochastic and independent) (van Kampen, 1981). The finding of the length independence of the motional diffusion coefficient thus provides evidence for the presence of correlation in the fluctuation in the microtubule sliding movement generated by kinesin in vitro. This places constraint on the possible molecular

Received for publication 1 May 1995 and in final form 30 October 1995.

Address reprint requests to Dr. K. Tawada, Department of Biology, Faculty of Science, Kyushu University, Fukuoka, Fukuoka 812, Japan. Tel. and Fax: 81-92-632-2742; E-mail: ktawascb@mbox.nc.kyushu-u.ac.jp.

© 1996 by the Biophysical Society

0006-3495/96/02/878/09 \$2.00

mechanisms of the sliding movement in vitro as will be discussed below. Some of these results have been briefly reported to the Seventh Biophysical Discussions on Molecular Motors (Tawada et al., 1995).

## MATERIALS AND METHODS

### Proteins

We prepared kinesin from bovine brains using DEAE-cellulose and phosphocellulose chromatography, followed by microtubule affinity and sucrose density centrifugation (Hackney, 1991). We prepared tubulin from porcine brains by two cycles of temperature-dependent polymerization, followed by phosphocellulose chromatography (Mitchison and Kirschner, 1984). Microtubules were polymerized in the presence of 9% dimethylsulfoxide and then stabilized with 40  $\mu$ M taxol (Vale and Toyoshima, 1988).

### Motility assays in vitro

We performed the kinesin motility assay using a microscope perfusion chamber at 25°C. We first infused kinesin of 6.25, 25, or 100  $\mu$ g/ml, supplemented with 0.2 mg/ml casein, into the chamber. After 3 min, unbound proteins were washed away by perfusing an assay buffer containing 10 mM Tris-acetate (pH 7.5), 50 mM potassium acetate, 4 mM  $\text{MgSO}_4$ , 1 mM EGTA, and 1 mM dithiothreitol. Microtubules (30  $\mu$ g/ml) and 1 mM ATP were then perfused into the chamber in the assay buffer.

We examined the microtubule movement over kinesin attached to a glass surface by dark field microscopy using a Nikon microscope equipped with a 100-W mercury light source, a heat filter, an Olympus dark field condenser (1.2–1.33 N.A.), and a Nikon 40 $\times$  objective lens. We took images of the filaments with an SIT camera (Ikegami CTC-9000) and recorded their movements onto a videocassette tape recorder.

### Data collection

We connected a videocassette tape recorder (SONY EVO-9650) to a video image digitizer board (I-O DATA, Kanazawa, Japan) in an Epson microcomputer (PC-486GR), and we controlled the operation of the video tape recorder through an RS232C circuit by custom software (written with C++) running on the microcomputer. By transferring the video images played back from the video tape recorder to the computer, we then displayed the images on the computer screen frame by frame. We next entered the  $x$ ,  $y$  coordinate position of microtubule ends (usually of their front tip) into the Epson computer, using a mouse-driven video cursor on the screen. The digitization accuracies for the  $x$  and  $y$  coordinates were 145 and 131 nm/pixel, respectively. The sampling interval for the data collection was 0.1 s. We usually collected approximately 200 digitized data points from a single trajectory of sliding movements in vitro.

### Calculation of the mean-square deviation of the sliding displacement from the average

We calculated this mean-square deviation, the variance of the sliding displacement, by

$$F_r^2 = \langle (r(\Delta t) - \langle r(\Delta t) \rangle)^2 \rangle \quad (1)$$

$$= 2D_m\Delta t, \quad (2)$$

where  $r(\Delta t)$  is the net displacement of a filament along its trajectory during a given time interval ( $\Delta t$ ), and  $\langle \rangle$  shows the average. Equation 2 yields a coefficient,  $D_m$ , which is referred to in this study as the motional diffusion coefficient. When the position measurement errors are present, the right-hand side of Eq. 2 has an additional term due to the errors (see below).

The net displacement,  $r(\Delta t)$ , along a trajectory in a time interval between  $t_j$  and  $t_{j+k}$  ( $\Delta t = t_{j+k} - t_j$ ;  $j = 0, 1, 2, \dots$  and  $k = 1, 2, 3, \dots$ ) was calculated by one of the following two methods.

1) Under the assumption that a trajectory is linear, the displacement is given by the distance between the two end points along the trajectory as

$$r(\Delta t) = \sqrt{[x(\Delta t)]^2 + [y(\Delta t)]^2} \quad (3)$$

where  $x(\Delta t) = x(t_{j+k}) - x(t_j)$  and  $y(\Delta t) = y(t_{j+k}) - y(t_j)$ ;  $x(t)$  and  $y(t)$  are the  $x$ ,  $y$  coordinates of a microtubule position. The distance thus calculated will be referred to as the linear distance between the two end points. Note that this method can only be applied to linear trajectories.

2) The net displacement is given by the contour length along a trajectory. To obtain the contour length we first smoothed a noisy trajectory (see below) and then summed each distance between two adjacent data points consecutively along a smoothed trajectory as

$$r(\Delta t) = \sum dr(t_{j+m+1}, t_{j+m}) \quad (m = 0 \text{ to } k-1) \quad (4)$$

where

$$dr(t_{j+m+1}, t_{j+m}) = \gamma \times \sqrt{[dx(t_{j+m+1})]^2 + [dy(t_{j+m+1})]^2}$$

with  $dx(t_{j+m+1}) = x(t_{j+m+1}) - x(t_{j+m})$  and  $dy(t_{j+m+1}) = y(t_{j+m+1}) - y(t_{j+m})$ , where  $\gamma$  is +1 for the forward movement and -1 for the backward movement along a smooth trajectory. The direction of the movement between  $t_{j+m+1}$  and  $t_{j+m}$  was determined by examining the sign of the scalar product of two vectors, one connecting the two positions at  $t_{j+m}$  and  $t_{j+m+1}$  and another from the position at  $t_{j+m}$  and the position a few (usually eight) data points ahead or behind along a trajectory. As the sampling interval for digitizing the position is set large enough,  $\gamma$  is usually positive. The distance thus calculated with Eq. 4 gives the contour length along a smoothed trajectory for a time interval  $\Delta t$  and will be referred to as the summed distance. This second method can be applied to curved as well as linear smoothed trajectories.

For the average calculations in Eq. 1 we used the following two methods: 1) an average calculation within a single trajectory of a filament (Qian et al., 1991), which is referred to in this study as single trajectory averaging, and 2) an average calculation over many filaments having lengths within a certain range, which is referred to as multiple trajectory averaging.

Position measurement errors were evaluated by the following two methods.

1) With the lengths of a microtubule image measured on many different frames on the computer screen, we calculated the variance of the length. This variance provides an estimate for the position measurement errors as explained below. The length ( $L$ ) of a microtubule image is given by

$$L = \sqrt{[(\Delta x)]^2 + [(\Delta y)]^2}, \quad (5)$$

with  $\Delta x = x_f - x_b$  and  $\Delta y = y_f - y_b$ , where  $x_f$  and  $y_f$  are the  $x$  and  $y$  coordinates of the front tip position of a microtubule and  $x_b$  and  $y_b$  are the  $x$  and  $y$  coordinates of the back tip of the filament. The variance of the measured length (Bevington and Robinson, 1992) is given by

$$\sigma_L^2 = (\partial L / \partial \Delta x)^2 \sigma_{\Delta x}^2 + (\partial L / \partial \Delta y)^2 \sigma_{\Delta y}^2 = \sigma_{\Delta x}^2 \text{ (or } \sigma_{\Delta y}^2), \quad (6)$$

where we assumed that  $\sigma_{\Delta x}^2 \approx \sigma_{\Delta y}^2$  because the digitization accuracy for the  $x$  and  $y$  coordinates is approximately the same as described above. As  $\Delta x$  is given by the difference between two measured  $x$  positions, we have  $\sigma_{\Delta x}^2 = 2\sigma_x^2$ , where  $\sigma_x^2$  is the variance of the digitization errors along an  $x$  axis. Similarly we have  $\sigma_{\Delta y}^2 = 2\sigma_y^2$ . We hence obtain

$$\sigma_x^2 \text{ (or } \sigma_y^2) = \sigma_L^2 / 2. \quad (7)$$

Therefore, the variance of the length measurement provides an estimate for the digitization errors ( $\sigma_x$  or  $\sigma_y$ ).

2) From the plot of the variance of the sliding distance versus the time interval, we estimated the position measurement errors. The principle of the second method is explained below.

Because there is a random error in the data collection of microtubule positions, unprocessed data for the linear distance obtained with Eq. 3 contains random errors. When such unprocessed data are used, the variance of the distance defined by Eq. 1 has a term due to the measurement errors, in addition to a term due to the intrinsic fluctuation in the sliding motion generated by kinesin, and we have

$$F_r^2 = \langle (r(\Delta t) - \langle r(\Delta t) \rangle)^2 \rangle \quad (8)$$

$$= 2D_m \Delta t + \sigma_{er}^2$$

where  $\sigma_{er}^2$  is the variance of the distance measurement errors (Bevington and Robinson, 1992; Imafuku et al., 1995; Qian et al., 1991). As the linear sliding distance is given by the distance between two positions on the computer screen, the variance of the distance measurement errors in Eq. 8 is related to the variance of the digitization errors as

$$\sigma_x^2 \text{ (or } \sigma_y^2) = \sigma_{er}^2/2. \quad (9)$$

as is  $\sigma_L^2$  in Eq. 7. Equations 8 and 9 lead to

$$F_r^2 = \langle (r(\Delta t) - \langle r(\Delta t) \rangle)^2 \rangle \quad (10)$$

$$= 2D_m \Delta t + 2\sigma_x^2 \text{ (or } 2\sigma_y^2).$$

As Eqs. 8 and 10 show, the variance of the sliding distance will increase linearly with the increase in the time interval above a constant term. This second constant term provides an estimate for the digitization errors along an  $x$  (or  $y$ ) axis,  $\sigma_x$  (or  $\sigma_y$ ). Note that one-half of the slope of the plot of Eq. 8 or 10 as a function of time yields the motional diffusion coefficient, whereas the intercept on the ordinate yields the digitization errors.

## Smoothing of the trajectories

Because the trajectories were noisy and usually not linear, it was not always possible to conduct single trajectory averaging. We therefore smoothed the trajectories for this average calculation by use of the following method. Each trajectory consists of two time series, the  $x$  and  $y$  coordinates as a function of time. We first smoothed each of the time series, using low-pass filtering in a frequency domain with a Hann window at 0.5 Hz, and then we reconstructed the smooth trajectory with the smoothed  $x$  and  $y$  coordinates as a function of time (Press et al., 1989). The proper cutoff frequency for the smoothing was chosen by examining the fast Fourier transform power spectra of the time series. The smoothing does not significantly affect either the fluctuation or the steady characteristics inherent to the filament sliding movements by protein motors *in vitro* as we have shown by a Monte Carlo study (Imafuku et al., 1995).

## RESULTS

Fig. 1 A shows a digitized trajectory of a microtubule sliding over kinesin. The unprocessed trajectory is noisy because of the errors arising from the digitization of the microtubule position on the computer screen. From an almost linear, unprocessed trajectory of a microtubule (the inset in Fig. 2), we measured its sliding displacements for various given time intervals and calculated the deviation of the sliding displacements from the average as a function time (Fig. 2). Fig. 2 shows that the sliding displacement deviation from the average fluctuates with an amplitude growing with time. As will be shown below, 1) the fluctuation consists of two different terms, one due to the position measurement errors and another that is inherent to the sliding motion, and 2) the

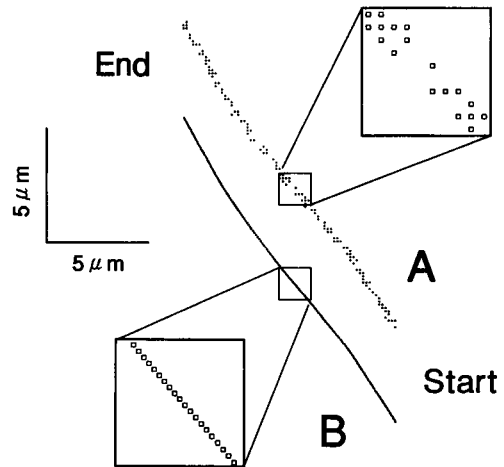


FIGURE 1 An example of the trajectories of a microtubule sliding over kinesin (25  $\mu\text{g/ml}$ ) attached to a glass surface at 25°C. The microtubule length was  $3.36 \pm 0.17 \mu\text{m}$  (mean  $\pm$  SD;  $N = 33$  different frames). (A) The original digitized trajectory before smoothing, consisting of 171 positional data points collected with a sampling interval of 0.1 s. (B) The trajectory after smoothing by low-pass filtering at a 0.5-Hz cutoff frequency as described in Materials and Methods, consisting of the same number of positional data points as in A.

amplitude of the former is time independent whereas that of the latter grows with time.

The position measurement errors due to digitization can be estimated from the standard deviation of the length measurement of microtubule images (see Eq. 7). From the value given in the legend to Fig. 1 and with Eq. 7, the standard deviation of the digitization errors along an  $x$  (or  $y$ )

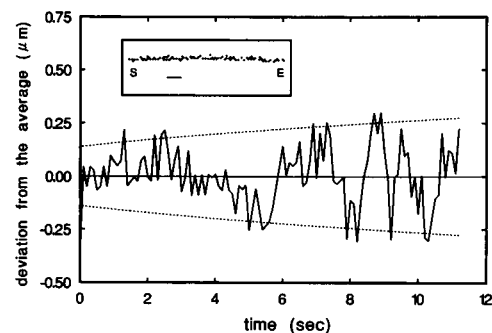


FIGURE 2 The fluctuation in the sliding displacement of a microtubule as shown by the displacement deviation from the average as a function of time (25°C; microtubule length, 16.7  $\mu\text{m}$ ; kinesin concentration, 100  $\mu\text{g/ml}$ ). The sliding displacement for a given time interval,  $r(\Delta t)$ , was obtained by measuring the linear distance between the initial point (time 0) to another point corresponding to the time interval. From all of the distances thus obtained from a single trajectory (shown in the inset), we first calculated the average drift velocity,  $\langle v \rangle$ , by using the values of  $r(\Delta t)/\Delta t$  and then calculated the displacement deviation from the average for various time intervals by  $r(\Delta t) - \langle v \rangle \Delta t$ . The motional diffusion coefficient of the microtubule was  $2.5 \times 10^{-11} \text{ cm}^2/\text{s}$  (see Materials and Methods). The dotted line is  $\pm \sqrt{(2D_m \Delta t + \sigma_{er}^2)}$  (from Eq. 8) with  $D_m = 2.6 \times 10^{-11} \text{ cm}^2/\text{s}$  and  $\sigma_{er} = 140 \text{ nm}$  (see below and Discussion). The inset shows the sliding trajectory consisting of 114 positional data points. S, start of the trajectory; E, end; bar, 1  $\mu\text{m}$ .

axis was found to be approximately 120 nm. The digitization errors can also be estimated from the plot of the mean-square deviation of sliding displacement from the average as a function of time, as will be described shortly.

A measure of the fluctuation inherent to the sliding motion is given by the motional diffusion coefficient. As described in Materials and Methods, the mean-square displacement deviation from the average as a function of time yields the motional diffusion coefficient. The main concern in this study has been to examine the dependence of the motional diffusion coefficients of microtubules on their filament length. To do so precisely, we needed to collect data of the motional diffusion coefficients for microtubules with various lengths. In this regard, the single trajectory averaging has an advantage over the multiple trajectory averaging (see Materials and Methods for these averaging methods), because the former, unlike the latter, yields a motional diffusion coefficient for each individual microtubule. In principle, multiple trajectory averaging can yield a motional diffusion coefficient of the microtubule for a given length, provided that we can collect positional data with a sufficiently large number of microtubules having the same length. In practice, however, this is very difficult. Therefore, we mainly used the single trajectory averaging.

Noise needs to be removed from trajectories such as that shown in Fig. 1 A for calculating the single trajectory averaging with the summed distances (see Materials and Methods). Hence we smoothed the trajectory by low-pass filtering as described in Materials and Methods. Fig. 1 B shows the resulting smoothed trajectory. Although the distances between the adjacent positional points along the smoothed trajectory appear to be almost homogeneous, the smoothed trajectory retains the fluctuation characteristics inherent to the sliding movement as described in Materials and Methods.

Fig. 3 A shows an example of the mean-square displacement deviation from the average as a function of time, for the calculation of which we used single trajectory averaging. There is a lag in the graph at small time intervals. The lag is a result of the smoothing with low-pass filtering (Imafuku et al., 1995). After the lag, there is a linear portion in the graph, as shown by the line. The motional diffusion coefficient of the sliding single filament is given by one-half of the linear slope (see Eq. 2 in Materials and Methods). The motional diffusion coefficient thus determined from this figure was  $5.6 \times 10^{-11} \text{ cm}^2/\text{s}$  for a microtubule of  $3.36 \mu\text{m}$ .

The breakdown in the linearity at a long time interval is not due to the vanished correlation but due to the increase in statistical errors. This is expected to ultimately occur in this sort of graph. In this average calculation, we take the average over all of the data positions of a single trajectory. Operationally, we take a set of calipers set for a fixed time interval and move the beginning point sequentially from the first position to the second position and so on along a trajectory. As the data number in a set of calipers for the average calculation is larger for a longer time interval, the number of independent data points available from a single

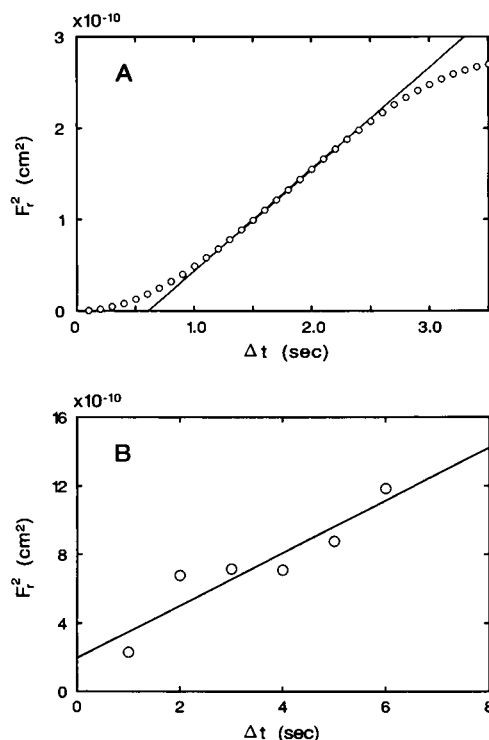


FIGURE 3 The mean-square displacement deviation from the average as a function of time interval. (A) Calculated by single trajectory averaging within a single trajectory of a  $3.36\text{-}\mu\text{m}$  microtubule (shown in Fig. 1 B), as described in Materials and Methods. We obtained the filled line using the linear regression method, following Uyeda et al. (1991). Half of the slope yields a value of  $5.6 \times 10^{-11} \text{ cm}^2/\text{s}$  for the motional diffusion coefficient. The size of the linear range depends on the total number of data available from a single trajectory and is larger when the number of data is greater. (B) Calculated by multiple trajectory averaging over 20 different trajectories of microtubules as described in Materials and Methods. The length range of the 20 microtubules was  $1.0\text{--}4.0 \mu\text{m}$  with an average of  $3.0 \mu\text{m}$ . The kinesin concentration was  $25 \mu\text{g/ml}$ . The linear regression line as shown by the filled line is given by  $F_r^2 = (1.53 \pm 0.26) \times 10^{-10} \times \Delta t + (1.96 \pm 0.44) \times 10^{-10}$  (Bevington and Robinson, 1992), therefore yielding a value of  $(7.7 \pm 1.3) \times 10^{-11} \text{ cm}^2/\text{s}$  for the motional diffusion coefficient. The square root of the second term on the right-hand side of this equation is  $1.4 \times 10^{-5} \text{ cm}$  (see the text and Eq. 10).

trajectory is smaller and therefore the statistical errors increase over a longer time interval (Qian et al., 1991; Lee et al., 1991).

For comparison, we calculated the mean-square displacement deviation from the average with multiple trajectory averaging (Fig. 3 B). For the average calculation we collected the data of the linear distance between the two end points (see Materials and Methods) from unsmoothed, linear trajectories. The line in Fig. 3 B is a regression line. The motional diffusion coefficient for a set of microtubules is given by 0.5 times the slope. The motional diffusion coefficient thus determined was  $7.7 \times 10^{-11} \text{ cm}^2/\text{s}$  for the microtubules with an average length of  $3.0 \mu\text{m}$ . This is close to the value obtained for a  $3.36\text{-}\mu\text{m}$  microtubule with single trajectory averaging ( $5.6 \times 10^{-11} \text{ cm}^2/\text{s}$ ) in Fig. 3 A.

The regression line in Fig. 3 B does not pass through the origin of the graph because of the digitization errors present

in the data. As the digitization errors are random, the line shifts upwards by a factor of two times the mean square of the errors (see Eq. 10). The square root of the intercept on the ordinate in Fig. 3 *B* was found to be 140 nm. From this value and Eq. 10, we obtained 100 nm for the standard deviation of the digitization errors, which is consistent with an error estimate made from the microtubule length measurement described above. Both estimates are thus close to the digitization accuracy for the *x* and *y* coordinates per pixel in our experiments (see Materials and Methods).

Fig. 4 shows the dependence of the motional diffusion coefficients on the microtubule length at three different kinesin concentrations. Here we used single trajectory averaging to obtain the motional diffusion coefficients. The relationship between the motional diffusion coefficient and the microtubule length depends upon the kinesin concentration. At the lowest kinesin concentration used (asterisks),

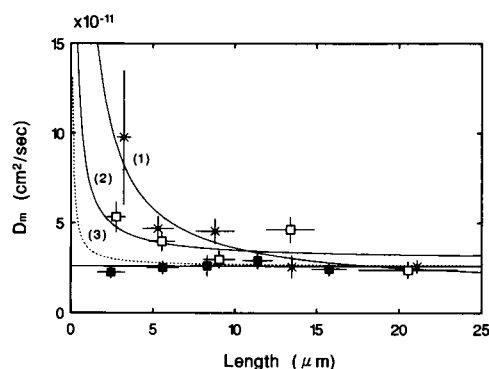


FIGURE 4 The motional diffusion coefficients versus the microtubule length at three different kinesin concentrations. Single trajectory averaging was used for the determination of the coefficients. There are 173 data points in total for the figure. It is not appropriate to show all of the individual data points because of the scatter. Hence, data for certain sets of microtubules were grouped and the averages are shown as follows. (\*) Kinesin concentration, 6.25  $\mu\text{g/ml}$ ; 60 different microtubules in total. The data points from the left show the average taken over the motional diffusion coefficients for 8 different microtubules in the range of 1–4  $\mu\text{m}$  (shown as  $N = 8$ , 1–4  $\mu\text{m}$ ;  $N = 15$ , 4–7  $\mu\text{m}$ ;  $N = 16$ , 7–11  $\mu\text{m}$ ;  $N = 10$ , 11–16  $\mu\text{m}$ ; and  $N = 11$ , >16  $\mu\text{m}$ ). (□) Kinesin concentration, 25  $\mu\text{g/ml}$ ; 55 different microtubules in total. The data points from the left show the average taken over the motional diffusion coefficients for microtubules of  $N = 10$ , 1–4  $\mu\text{m}$ ;  $N = 12$ , 4–7  $\mu\text{m}$ ;  $N = 12$ , 7–11  $\mu\text{m}$ ;  $N = 10$ , 11–16  $\mu\text{m}$ ; and  $N = 11$ , >16  $\mu\text{m}$ . (■) Kinesin concentration, 100  $\mu\text{g/ml}$ ; 58 different microtubules in total. The data points from the left show the average taken over the motional diffusion coefficients for microtubules of  $N = 16$ , 1–4  $\mu\text{m}$ ;  $N = 16$ , 4–7  $\mu\text{m}$ ;  $N = 7$ , 7–10  $\mu\text{m}$ ;  $N = 11$ , 10–14  $\mu\text{m}$ ; and  $N = 8$ , >14  $\mu\text{m}$ . The horizontal filled line shows the average of the closed square data ( $2.6 \times 10^{-11} \text{ cm}^2/\text{s}$ ). The ordinate values indicate the mean  $\pm$  SEM (for  $N$  shown above), whereas the abscissa values indicate the mean  $\pm$  SD (for  $N$  shown above). The curve (1) shows a nonlinear regression line of Eq. A3 (equivalent to Eq. 11) fitted directly to all of the original 60 data points (not shown) at the 6.25- $\mu\text{g/ml}$  kinesin concentration. The curve (2) shows a nonlinear regression line of Eq. A3 (Eq. 11) fitted directly to all of the original 55 data points (not shown) at the 25- $\mu\text{g/ml}$  kinesin concentration. For the regression, the simplex method (Press et al., 1989) was used. The curve (3) shows Eq. A3 (Eq. 11) calculated with estimated values for  $\zeta$  and  $D_{ac}$  as explained in the Appendix.

the motional diffusion coefficient decreases with increasing filament length and becomes independent of lengths  $\geq 13 \mu\text{m}$ . At the intermediate kinesin concentration (open squares), the motional diffusion coefficient depends upon the filament length, for lengths  $< 5 \mu\text{m}$ . At the highest kinesin concentration (filled squares), the motional diffusion coefficient does not depend on the filament length in the range we studied. The motional diffusion coefficients for long microtubules  $\geq 10 \mu\text{m}$  appear to have similar values for all three kinesin concentrations. The most surprising result in Fig. 4 is that the motional diffusion coefficient of the microtubules sliding over kinesin becomes independent of microtubule length at high kinesin concentrations. This result was confirmed by using multiple trajectory averaging (data not shown).

Fig. 5 shows the average sliding velocity of microtubules at three different concentrations of kinesin. The sliding velocity does not depend appreciably upon either the microtubule length or the kinesin concentration, as previously reported by Howard et al. (1989).

## DISCUSSION

By analyzing the trajectories of the microtubules sliding over kinesin in vitro, we have quantitatively characterized the fluctuation in the sliding (translational) motion. It should be pointed out that we analyzed the sliding motion of microtubules that was generated by many kinesin molecules (approximately 100 molecules per 1- $\mu\text{m}$  microtubule) in the conventional motility assay system. This is important because our results will be later discussed in terms of a theorem in the statistics.

Our fluctuation analysis approach produced motional diffusion coefficients, which are a measure of the fluctuation of the sliding motion. This coefficient has the following three major characteristics. 1) The motional diffusion coefficient is smaller than the longitudinal diffusion coefficient of a microtubule freely suspended in solution (Table 1). For

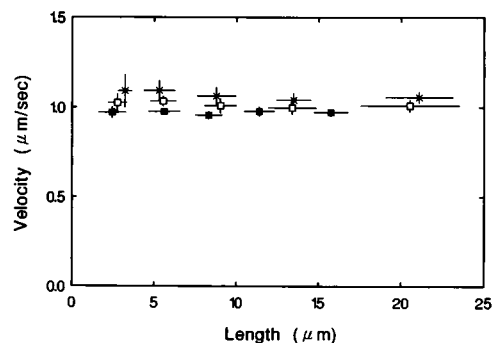


FIGURE 5 The average sliding velocities versus the microtubule length at three different kinesin concentrations. Single trajectory averaging was used for the determination of the average velocities. The symbols and conditions are the same as those in Fig. 4. Here data were grouped as in Fig. 4. Both the ordinate and abscissa values indicate the mean  $\pm$  SD (for  $N$  shown as in Fig. 4).

**TABLE 1** Diffusion coefficients of the microtubules undergoing either Brownian movement\* or sliding movement with fluctuation over kinesin<sup>‡</sup>

	Diffusion coefficient (cm <sup>2</sup> /s)	Length ( <i>L</i> ) dependence	References
Free diffusion*	$1.9 \times 10^{-8}$	1/ <i>L</i>	Berg, 1993
Over dynein*	$3.3 \times 10^{-10}$	1/ <i>L</i>	Vale et al., 1989
Over <i>ncd</i> mutant*	$1.5 \times 10^{-9}$	1/ <i>L</i>	Chandra et al., 1993
Over dynamin*	$1.3 \times 10^{-11}$	ND	Nataka et al., 1993
In methylcellulose*	$2.2 \times 10^{-11}$	ND	Nakata et al., 1993
Over kinesin <sup>‡</sup>	$2.6 \times 10^{-11}$	No dependence	This work

\*The longitudinal diffusion coefficients for a 1.5- $\mu$ m microtubule.

<sup>‡</sup>The average of the motional diffusion coefficients at the kinesin concentration of 100  $\mu$ g/ml shown in Fig. 4.

ND, not determined.

example, the motional diffusion coefficient of the microtubules at the highest kinesin concentration was  $2.6 \times 10^{-11}$  cm<sup>2</sup>/s. This value is approximately 1/800 of the latter diffusion coefficient for a microtubule of 1.5  $\mu$ m ( $1.9 \times 10^{-8}$  cm<sup>2</sup>/s). 2) The motional diffusion coefficient at the lowest and intermediate kinesin concentrations (6.25 and 25  $\mu$ g/ml) depended upon the microtubule length; the coefficient decreased (but did not go down asymptotically to zero) with increasing the filament length (Fig. 4). 3) The motional diffusion coefficient at the highest kinesin concentration did not depend upon the microtubule length in the range we studied (Fig. 4).

The above third characteristic is not an artifact due to our smoothing method, because we obtained the same result with unsmoothed trajectory data as described in Results. This is substantiated by our observation that the fast Fourier transform power spectrum of an unprocessed positional time series of a short (2.6- $\mu$ m) microtubule is almost the same as that of a long (15.7- $\mu$ m) microtubule at the kinesin concentration of 100  $\mu$ g/ml (data not shown). As the digitization errors are length independent, the reader may wonder whether such digitization errors affect the determination of  $D_m$ . As explained in Results (Fig. 3 B) and Materials and Methods (see Eqs. 8 and 10), the slope of the plot such as that shown in Fig. 3 B yields  $D_m$ , whereas the intercept on the ordinate of the plot yields the digitization errors. Therefore, the digitization errors do not significantly affect the determination of  $D_m$ . The digitization errors estimated from Fig. 3 B are consistent with those estimated from the variance of the microtubule length measurement as described in Results. With an estimate of the digitization errors obtained from Fig. 3 B and a value for  $D_m$  shown in Table 1, we plotted  $\pm\sqrt{\text{Eq. 8}}$  in Fig. 2 (dotted lines). Equation 8 with these parameter values is thus consistent with the fluctuation with a growing amplitude shown in Fig. 2.

Microtubules undergo one-dimensional, random Brownian movement when they are placed over dynein in the presence of vanadate (a dynein ATPase inhibitor) plus ATP (Vale et al., 1989), over an amino-terminal truncated mutant of the *ncd* motor protein in the presence of ATP (Chandra et

al., 1993), over dynamin in a mixture of ATP/GTP, or in methylcellulose (Nakata et al., 1993). The longitudinal diffusion coefficient of a microtubule of 1.5  $\mu$ m under these conditions is approximately  $10^{-11} \sim 10^{-9}$  cm<sup>2</sup>/s (Table 1). This value is, as is the motional diffusion coefficient obtained by us here, much smaller than the diffusion coefficients of the microtubules freely suspended in solution ( $1.9 \times 10^{-8}$  cm<sup>2</sup>/s for a 1.5- $\mu$ m microtubule). The diffusion coefficient is related to the inverse of the friction coefficient. A small value for the diffusion coefficient indicates the presence of a large friction coefficient. We previously explained the relatively small diffusion coefficient of the microtubules undergoing Brownian movement over dynein in vanadate plus ATP, by a protein friction model (Tawada and Sekimoto, 1991b). In the Appendix, we analyze the length dependence of  $D_m$  in terms of the protein friction model.

As shown in the Appendix, we can approximate all the data shown in Fig. 4 by an equation (Eq. A3 in the Appendix):

$$D_m = kT/(L\zeta) + D_{ac}, \quad (11)$$

where  $k$  is the Boltzmann constant,  $T$  is the absolute temperature,  $L$  is the microtubule length,  $\zeta$  is the friction coefficient per unit length of the filament, and  $D_{ac}$  is a term due to the fluctuation in the active sliding force, a term that is assumed to be length independent. By fitting Eq. 11 to the data in Fig. 4, we obtained a value of 2–40 g/s/cm for  $\zeta$  (Table 2). The value in this range is more than 100 times larger than the coefficient of the solvent friction and is thus consistent with a value previously estimated for the protein friction (Tawada and Sekimoto, 1991a,b). The protein friction with such a large coefficient was proposed to be operating as a velocity-limiting factor in the sliding motion in vitro (Tawada and Sekimoto, 1991a).

The presence of the protein friction also indicates that the Brownian movement of the microtubules observed by Vale et al. (1989) is not directly driven by the atomic collision of the solvent molecules but is driven by the thermally generated structural fluctuations of dynein motors that interact with the microtubules with a weak binding interaction (Tawada and Sekimoto, 1991b). This means that dynein motors in this system can generate a temporarily transla-

**TABLE 2** Estimated values of parameters in Eq. 11 (Eq. A3)

Kinesin concentrations ( $\mu$ g/ml)	$\zeta$ (g/s/cm)	$D_{ac}$ (cm <sup>2</sup> /s)
6.25	1.9	$1.4 \times 10^{-11}$
25	8.6	$3.0 \times 10^{-11}$
100	40*	$2.6 \times 10^{-11\ddagger}$

See Appendix for the estimation.

\*Estimated from the other two values as described in the Appendix.

<sup>‡</sup>Assumed to be equal to the average of  $D_m$  at the kinesin concentration of 100  $\mu$ g/ml in Fig. 4. The coefficient of the solvent friction for a microtubule is  $1.6 \times 10^{-2}$  g/s/cm (Berg, 1993). The temperature ( $T$ ) in Eq. 11 was 300 K.

tional, random movement of a microtubule without ATP splitting; naturally, the movement in this case is not unidirectional because the energy of ATP hydrolysis is not supplied.

As the protein friction is larger at larger kinesin concentrations, the first term on the right-hand side of Eq. 11 becomes smaller at larger kinesin concentrations and hence contributes little to  $D_m$  at the highest kinesin concentration. Under this condition,  $D_{ac}$ , the length-independent component, accordingly remains dominant. This is a phenomenological explanation for the length independence of  $D_m$  observed at the highest kinesin concentration, in terms of Eq. 11.

The curve fitting of Eq. 11 to the data in Fig. 4 also yielded values for  $D_{ac}$ . These were  $1.4 \times 10^{-11}$  and  $3.0 \times 10^{-11}$  cm<sup>2</sup>/s for 6.25 and 25  $\mu$ g/ml kinesin concentrations, respectively. The value of  $D_{ac}$  at the highest kinesin concentration (100  $\mu$ g/ml) is not known but may be close to the average of  $D_m$  at this concentration, as indicated by the observation that Eq. 11 at the kinesin concentration (broken line) is close to the horizontal filled line showing the average  $D_m$ , except at small lengths (Fig. 4). Although the kinesin concentration was varied 16-fold,  $D_{ac}$  varied only by a factor of approximately two, and furthermore, no systematic changes were observed in the variation of  $D_{ac}$  (Table 2).

The length independence of  $D_m$  at the highest kinesin concentration is a surprising finding. Before discussing the significance of this finding, we will first consider the length dependence of the Brownian movement of microtubules. The diffusion coefficient is a measure of the positional fluctuation of a Brownian particle (Berg, 1993). The longitudinal diffusion coefficient of a microtubule undergoing Brownian movement is approximately proportional to the inverse of the microtubule length. This is so in solution as well as in the protein environments mentioned above (Table 1). This inverse proportionality is a direct consequence of the central limit theorem with the premise that the action of the particles causing Brownian movement is random (i.e., stochastic and independent) (van Kampen, 1981); the fluctuation is relatively smaller with a larger number of particles randomly involved in the motion, thus smaller for longer filaments. As the directional sliding motion of a microtubule is generated by the action of many kinesin molecules in our experiments, we could expect that the motional diffusion coefficient, a measure of the fluctuation of the sliding displacement from the average, would be likewise proportional to the inverse of the microtubule length. As is shown in Fig. 4, however, this was not the case at a sufficiently high kinesin concentration. Therefore, the premise of the central limit theorem appears to be violated in the directional sliding movements *in vitro*.

In parallel with this study, we have also been analyzing the fluctuation of the sliding movements of either microtubules driven by sea urchin dynein or actin driven by heavy meromyosin from rabbit skeletal muscle. In parallel experiments with these other systems, we have found a similar length independence of the motional diffusion coefficient

(Imafuku et al., unpublished results). The length independence of the motional diffusion coefficient thus is genuine in the *in vitro* sliding movements of cytoskeletal filaments driven by protein motors in general.

There are several possible explanations for the length independence of  $D_m$  observed at the highest kinesin concentration. For example, it is possible that a cooperative action between or among kinesin heads exists in causing the sliding movement. Recent reports clearly showed the existence of such cooperativity between the two heads of a kinesin molecule (Gilbert et al., 1995; Berliner et al., 1995). If this explanation is the case, we must suppose the existence of a similar cooperativity between or among the heads of myosin and also between or among those of dynein, because a similar length independence of  $D_m$  was found with these latter two protein motors. Although the heads of myosin are usually considered to act independently, this is not proven (Schnapp, 1995). This independent action may be the case at the isometric condition (see below) but is not proven when there is a translational sliding movement between a filament and protein motors.

With regard to the cooperativity, it is noted that sliding movements generated by a single motor molecule such as those reported by Howard et al. (1989), Hunt and Howard (1993), Svoboda et al. (1993; 1994), and Berliner et al. (1995) were all generated by a single motor molecule with two heads, not by a single motor molecule with one head. These observations suggest that the generation of the translational sliding movement of a filament requires at least two subunits of motor proteins. The reasons for this requirement may be geometrical as well as dynamical. The premises of the central limit theorem are usually violated in dynamical systems operating far away from equilibrium, where nonlinear dynamics play a key role (Nicolis and Prigogine, 1989). The motility system consisting of a filament and more than two subunits of motor proteins, which generates the sliding movement by using the energy of ATP hydrolysis (thus operating away from equilibrium), can be such a dynamical system, and therefore nonlinear dynamics play a key role in the sliding movement generation. In this regard, it would be interesting to analyze the fluctuation of the sliding motion and related phenomena with various techniques that have recently developed in nonlinear science (Kaplan and Glass, 1995).

An alternative possible explanation is to consider the heterogeneity in the distribution of kinesin on the glass surface in the *in vitro* motility assay system and to suppose that the effectiveness of the action of individual kinesin heads in causing the sliding motion varies from head to head because of their spatial heterogeneity relative to the direction of a sliding microtubule. As the action of a given kinesin head continually lasts for a time interval approximately equivalent to the ratio of the microtubule length over the sliding velocity, the microtubule sliding motion has a temporal correlation for this time interval. The central limit theorem cannot be applied to a system with such a temporal correlation, and thus the fluctuation of the sliding motion

can be insensitive to the length of the microtubule. In fact, a theoretical modeling of the second possibility has shown that the motional diffusion coefficient does not depend upon the filament length (Sekimoto and Tawada, 1995). The theoretical modeling has shown that  $D_m$  ( $D_{ac}$  in Eq. 11 to be more precise) is approximately equal to the ratio of the average sliding velocity over the number of kinesin heads per unit length of microtubule that can interact with the filament.

The above second possibility may be checked by examining the movement of actin filaments sliding along a long myosin thick filament from molluscan smooth muscle (Sellers and Kachar, 1990; Yamada et al., 1990), in which the myosin heads are more uniformly oriented. To discriminate the above two possibilities, we need to make a theoretical model for the first possibility, which derives an equation for  $D_m$ , and compare these two theoretical results with experiments more quantitatively.

In contrast, the central limit theorem holds true in the isometric force generation in vitro by myosin. There, the relative force fluctuation is proportional to (average force) $^{-1/2}$  (Ishijima et al., 1991). Assuming that the force production is proportional to the number of myosin heads ( $N$ ) interacting with an actin filament, this finding shows that the relative force fluctuation is proportional to  $N^{-1/2}$  and therefore indicates that the central limit theorem holds true in this case. In other words, the premises of the central limit theorem are not violated when there is no translational movement between the cytoskeletal filament and the protein motors.

To sum up, the length independence of the motional diffusion coefficient observed at sufficiently high kinesin concentrations is a characteristic of a translational sliding movement. The length independence may offer some new insights to help further elucidate the physical processes behind the translational sliding movement generation by protein motors in vitro.

## APPENDIX

As shown in Fig. 4, the motional diffusion coefficient was observed to depend upon the microtubule length except at the highest kinesin concentration. We discuss this length dependence from the perspective of our previous protein friction model (Tawada and Sekimoto, 1991a,b).

Suppose a microtubule is caused to slide by kinesin in the presence of ATP. The filament is subjected to various forces with fluctuation, which include thermally generated forces and the active sliding force that is generated by kinesin by using the energy of ATP hydrolysis. Thus the filament motion has two components, thermal motion and active motion. The thermal motion is generated by the thermal collision of the solvent molecules with the filament and also by the thermal fluctuation of the protein structure of kinesin that cyclically attaches to, and subsequently detaches from, the microtubule without any concomitant ATP splitting (i.e., reversibly). The resulting thermal motion is a random process and thus contributes to the fluctuation in the sliding motion. We also note that the active sliding force generated by kinesin molecules fluctuates around an average. The fluctuation of the active force additionally contributes to the fluctuation of the sliding motion. Therefore, the fluctuation in the microtubule sliding motion is caused by these two different processes, each of which is independent of the other. Accordingly, the mean-square dis-

placement deviation from the average (a measure of the fluctuation) in the sliding motion consists of two terms due to these two different, independent processes. In other words, the motional diffusion coefficient ( $D_m$ ) is given as

$$D_m = D_{th} + D_{ac}, \quad (A1)$$

where  $D_{th}$  is the term due to thermally generated fluctuation and  $D_{ac}$  is the term due to the fluctuation of the active force.

When no active force is generated, we have

$$D_m = D_{th} = kT/(L\zeta) \quad (A2)$$

where  $k$  is the Boltzmann constant,  $T$  is the absolute temperature,  $L$  is the microtubule length and,  $\zeta$  is the protein friction per unit length of microtubule (Tawada and Sekimoto, 1991b). On the right-hand side of Eq. A2, we ignored the contribution of the solvent friction to  $D_{th}$  because  $D_m$  (and therefore  $D_{th}$ ) has been experimentally found to be much smaller than the diffusion coefficient of a microtubule freely suspended in solution (see the appendix of Tawada and Sekimoto, 1991b). From Eqs. A1 and A2, we have

$$D_m = kT/(L\zeta) + D_{ac}. \quad (A3)$$

The explicit form of a theoretical expression for  $D_{ac}$  depends upon a specific model on the interaction of kinesin with microtubules. Instead, we take a phenomenological approach to characterize  $D_{ac}$  in the light of the experimentally available data.

If we assume that  $D_{ac}$  is independent of the microtubule length, Eq. A3 is consistent with the  $D_m$  data in Fig. 4. As the protein friction ( $\zeta$ ) is larger at larger concentrations of kinesin (Tawada and Sekimoto, 1991b), the first term on the right-hand side of Eq. A3 is smaller at larger kinesin concentrations and can be smaller than the second term ( $D_{ac}$ ) at the highest kinesin concentration, thus leaving  $D_{ac}$  dominant. Below we will show that this interpretation is quantitatively consistent with the data in Fig. 4.

We fitted Eq. A3 to the data at the kinesin concentrations of 6.25 and 25  $\mu\text{g/ml}$  with the simplex method (Press et al., 1989). The fitted equations are shown by the filled curves in Fig. 4. A good fit was obtained. The fitting yielded values for  $\zeta$  and  $D_{ac}$  at these two kinesin concentrations, which are summarized in Table 2. From these two values of  $\zeta$ , we estimated a value for  $\zeta$  at the highest kinesin concentration (100  $\mu\text{g/ml}$ ) as follows to draw a curve of Eq. A3 at this kinesin concentration. As described above,  $\zeta$  is considered to be an increasing function of the kinesin concentration. To be more specific,  $\zeta$  is proportional to the number of kinesin molecules on a glass surface that can interact with a microtubule of a unit length ( $\rho$ ) (Tawada and Sekimoto, 1991b). Because we do not know the relationship between  $\rho$  and the kinesin concentration, we put  $\zeta = \zeta_0[\text{kinesin}]^n$  and fitted it to the data of  $\zeta$  at the two kinesin concentrations. By doing so, we found that  $\zeta$  is proportional to  $[\text{kinesin}]^{1.1}$ , with which we estimated a value for  $\zeta$  at the kinesin concentration of 100  $\mu\text{g/ml}$ . The estimated value is shown in Table 2. Assuming this value for  $\zeta$  together with an assumption that  $D_{ac}$  is equal to the average of  $D_m$  at the highest kinesin concentration, we drew Eq. A3 in Fig. 4 (broken line). At lengths  $\geq 5 \mu\text{m}$ , the line of Eq. A3 is almost flat and close to the experimental data at the highest kinesin concentration. Therefore we conclude that Eq. A3 is quantitatively consistent with the experimental data in Fig. 4.

We thank Ken Sekimoto for comments on this manuscript.

## REFERENCES

- Berg, H. C. 1993. *Random Walks in Biology*, Expanded Edition. Princeton University Press, Princeton. 48–64.
- Berliner, E., E. C. Young, K. Anderson, H. K. Mahtani, and J. Gelles. 1995. Failure of a single-headed kinesin to track parallel to microtubule protofilaments. *Nature (Lond)*. 373:718–721.



- Bevington, P. R., and D. K. Robinson. 1992. Data Reduction and Error Analysis for the Physical Sciences, 2nd ed. McGraw-Hill, New York. 96–114.
- Chandra, R., S. A. Endow, and E. D. Salmon. 1993. An N-terminal truncation of the *ncd* motor protein supports diffusional movement of microtubules in motility assays. *J. Cell Sci.* 104:899–906.
- Gilbert, S. P., M. R. Webb, M. Brune, and K. A. Johnson. 1995. Pathway of processive ATP hydrolysis by kinesin. *Nature (Lond.)* 373:671–676.
- Hackney, D. D. 1991. Isolation of kinesin using initial batch ion exchange. *Methods Enzymol.* 196:175–181.
- Harada, Y., A. Noguchi, A. Kishino, and T. Yanagida. 1987. Sliding movement of single actin filaments on one-headed myosin filaments. *Nature (Lond.)* 326:805–808.
- Howard, J., A. J. Hudspeth, and R. D. Vale. 1989. Movement of microtubules by single molecules. *Nature (Lond.)* 342:154–158.
- Hunt, A. J., and J. Howard. 1993. Kinesin swivels to permit microtubule movement in any direction. *Proc. Natl. Acad. Sci. USA.* 90: 11653–11657.
- Imafuku, Y., Y. Y. Toyoshima, and K. Tawada. 1996. Monte Carlo study for fluctuation analysis in the in vitro motility driven by protein motors. *Biophys. Chem.* 59:In press.
- Ishijima, A., T. Doi, K. Sakurada, and T. Yanagida. 1991. Sub-piconewton force fluctuation of actomyosin in vitro. *Nature (Lond.)* 352:301–306.
- Kaplan, D., and L. Glass. 1995. Understanding Nonlinear Dynamics. Springer-Verlag, New York. 279–358.
- Kron, S. J., and J. A. Spudich. 1986. Fluorescent actin filaments move on myosin fixed to a glass surface. *Proc. Natl. Acad. Sci. USA.* 83: 6272–6276.
- Lee, G. M., A. Ishihara, and K. A. Jacobson. 1991. Direct observation of Brownian motion of lipids in a membrane. *Proc. Natl. Acad. Sci. USA.* 88:6274–6278.
- Mitchison, T., and M. Kirschner. 1984. Microtubule assembly nucleated by isolated centrosomes. *Nature (Lond.)* 312:232–237.
- Nakata, T., R. Sato-Yoshitake, Y. Okada, Y. Noda, and N. Hirokawa. 1993. Thermal drift is enough to drive a single microtubule along its axis even in the absence of motor proteins. *Biophys. J.* 65:2504–2510.
- Nicolis, G., and I. Prigogine. 1989. Exploring Complexity. Freeman, New York. 147–192.
- Press, W. H., B. P. Flannery, S. A. Teukolsky, and W. T. Vetterling. 1989. Numerical Recipes in Pascal. Cambridge University Press, Cambridge. 459–462, 543–546.
- Qian, H., M. P. Sheetz, and E. L. Elson. 1991. Single particle tracking. *Biophys. J.* 60:910–921.
- Schnapp, B. J. 1995. Two heads are better than one. *Nature (Lond.)* 373:655–656.
- Sekimoto, K., and K. Tawada. 1995. Extended time correlation of in vitro motility by motor protein. *Phys. Rev. Lett.* 75:180–183.
- Sellers, J. R., and B. Kachar. 1990. Polarity and velocity of sliding filaments: control of direction by actin and of speed by myosin. *Science.* 249:406–408.
- Svoboda, K., P. P. Mitra, and S. M. Block. 1994. Fluctuation analysis of motor protein movement and single enzyme kinetics. *Proc. Natl. Acad. Sci. USA.* 91:11782–11786.
- Svoboda, K., C. F. Schmidt, B. J. Schnapp, and S. M. Block. 1993. Direct observation of kinesin stepping by optical trapping interferometry. *Nature (Lond.)* 365:721–727.
- Tawada, K., Y. Imafuku, and Y. Y. Toyoshima. 1995. A single-track fluctuation analysis in the sliding movement by protein motors in vitro. *Biophys. J.* 68:68s.
- Tawada, K., and K. Sekimoto. 1991a. A physical model of ATP-induced actin-myosin movement in vitro. *Biophys. J.* 59:343–356.
- Tawada, K., and K. Sekimoto. 1991b. Protein friction exerted by motor enzymes through a weak-binding interaction. *J. Theor. Biol.* 150: 193–200.
- Uyeda, T. P. Q., H. M. Warrick, S. J. Kron, and J. A. Spudich. 1991. Quantized velocities at low myosin densities in an in vitro motility assay. *Nature (Lond.)* 352:307–311.
- Vale, R. D., D. R. Soll, and I. R. Gibbons. 1989. One-dimensional diffusion of microtubules bound to flagellar dynein. *Cell.* 59:915–925.
- Vale, R. D., and Y. Y. Toyoshima. 1988. Rotation and translocation of microtubules in vitro induced by dyneins from tetrahymena cilia. *Cell.* 52:459–469.
- van Kampen, N. G. 1981. Stochastic Processes in Physics and Chemistry. North-Holland, Amsterdam. 253–283.
- Yamada, A., N. Ishii, and K. Takahashi. 1990. Direction and speed of actin filaments moving along thick filaments isolated from molluscan smooth muscle. *J. Biochem (Tokyo).* 108:341–343.